







Gene therapy targeting the blood–brain barrier improves neurological symptoms in a model of genetic MCT8 deficiency

Sivaraj M. Sundaram,^{1,†} Adriana Arrulo Pereira,^{1,†}  Helge Müller-Fielitz,¹ Hannes Köpke,¹ Meri De Angelis,^{2,3} Timo D. Müller,² Heike Heuer,⁴  Jakob Körbelin,^{1,5} Markus Krohn,¹  Jens Mittag,⁶ Ruben Nogueiras,⁷ Vincent Prevot⁸ and  Markus Schwaninger^{1,9}

[†]These authors contributed equally to this work.

A genetic deficiency of the solute carrier monocarboxylate transporter 8 (MCT8), termed Allan–Herndon–Dudley syndrome, is an important cause of X-linked intellectual and motor disability. MCT8 transports thyroid hormones across cell membranes. While thyroid hormone analogues improve peripheral changes of MCT8 deficiency, no treatment of the neurological symptoms is available so far. Therefore, we tested a gene replacement therapy in *Mct8*- and *Oatp1c1*-deficient mice as a well-established model of the disease. Here, we report that targeting brain endothelial cells for *Mct8* expression by intravenously injecting the vector AAV-BR1-*Mct8* increased tri-iodothyronine (T3) levels in the brain and ameliorated morphological and functional parameters associated with the disease. Importantly, the therapy resulted in a long-lasting improvement in motor coordination. Thus, the data support the concept that MCT8 mediates the transport of thyroid hormones into the brain and indicate that a readily accessible vascular target can help overcome the consequences of the severe disability associated with MCT8 deficiency.

- 1 Institute for Experimental and Clinical Pharmacology and Toxicology, Center of Brain, Behavior and Metabolism, University of Lübeck, 23562 Lübeck, Germany
- 2 Institute for Diabetes and Obesity, Helmholtz Zentrum Munich, Munich, and German Center for Diabetes Research (DZD), 85764 Neuherberg, Germany
- 3 Institute of Experimental Genetics, Helmholtz Zentrum Munich, German Research Center for Environmental Health (GmbH), 85764 Neuherberg, Germany
- 4 Department of Endocrinology, Diabetes and Metabolism, University Hospital Essen, University Duisburg-Essen, 45147 Essen, Germany
- 5 Department of Oncology, Hematology and Bone Marrow Transplantation, UKE Hamburg-Eppendorf, 20246 Hamburg, Germany
- 6 Institute for Endocrinology and Diabetes, Center of Brain, Behavior and Metabolism, University of Lübeck, 23562 Lübeck, Germany
- 7 Department of Physiology, CIMUS, University of Santiago de Compostela-Instituto de Investigación Sanitaria, 15782 Santiago de Compostela, Spain
- 8 Université Lille, Inserm, CHU Lille, Laboratory of Development and Plasticity of the Neuroendocrine Brain, Lille Neuroscience & Cognition, UMR-S 1172, European Genomic Institute for Diabetes (EGID), 59045 Lille Cedex, France
- 9 DZHK (German Research Centre for Cardiovascular Research), Hamburg-Lübeck-Kiel, Germany

Received December 8, 2021. Revised June 3, 2022. Accepted June 22, 2022. Advance access publication August 5, 2022

© The Author(s) 2022. Published by Oxford University Press on behalf of the Guarantors of Brain.

This is an Open Access article distributed under the terms of the Creative Commons Attribution-NonCommercial License (<https://creativecommons.org/licenses/by-nc/4.0/>), which permits non-commercial re-use, distribution, and reproduction in any medium, provided the original work is properly cited. For commercial re-use, please contact journals.permissions@oup.com

Correspondence to: Markus Schwaninger
Institute for Experimental and Clinical Pharmacology and Toxicology
University of Lübeck Ratzeburger Allee 160, 23562 Lübeck, Germany
E-mail: markus.schwaninger@uni-luebeck.de

Keywords: thyroxine; tri-iodothyronine; cretinism; myelination; hypothyroidism

Abbreviations: AAV = adeno-associated virus; AHDS = Allan–Herndon–Dudley syndrome; DKO = *Mct8* and *Oatp1c1* double knockout mice; PBECS = primary brain endothelial cells; T3 = tri-iodothyronine; T4 = thyroxine; TH = thyroid hormone

Introduction

The thyroid hormones (THs) thyroxine (T4) and tri-iodothyronine (T3) are critical for the function of the CNS. Severe hypothyroidism causes cognitive deficits and other neurological symptoms.^{1,2} Mild TH deficiency has been associated with major depression and dementia.^{3,4} In the CNS, nuclear receptors and deiodinases maintain TH homeostasis, but the initial step required for the action of THs is their cellular uptake by solute carriers. Among the latter family of proteins, monocarboxylate transporter 8 (MCT8) and organic anion transporter polypeptide 1c1 (OATP1C1) have been shown to transport THs *in vivo*.^{5,6} Mutations of the X-linked MCT8 gene (*SLC16A2*) cause severe intellectual disability, motor dysfunction and peripheral thyrotoxicosis (Allan–Herndon–Dudley syndrome, AHDS).^{7–10} It has been estimated that MCT8 mutations are responsible for almost 4% of all X-linked intellectual disabilities.¹¹ Affected boys appear normal at birth but show developmental delay and feeding problems in the first year of life. Some patients cannot fully control their head, speak or walk. Other motor symptoms include muscle weakness, gait ataxia and dystonia. The TH analogues 3,5-diiodothyropropionic acid (DITPA) and 3,3',5-triiodothyroacetic acid (TRIAC) improved the peripheral thyroid status,^{12,13} but treatment of the CNS symptoms that are key to patients' disabilities is still not available and represents an unmet medical need.

Neuropathological changes underlying symptoms of MCT8 deficiency include an altered cerebellar structure, lack of parvalbumin-positive interneurons, delayed myelination and oligodendrocyte dysfunction,¹⁴ indicative of a global TH deficiency in the CNS. Although MCT8 mutations severely affect oligodendrocytes and neurons in humans, these cells either do not contain significant amounts of MCT8 protein or produce it only during development or in subpopulations.^{15–17} Interestingly, brain barriers, including endothelial cells, express MCT8 into adulthood, pointing to a pivotal role of MCT8 in TH transport through the brain barriers.^{15,16}

Mouse studies support this hypothesis. Unlike human patients, *Mct8*^{-/-} mice do not show a neurological phenotype^{18,19}; in mice but not in humans, OATP1C1 functions as a second transporter in brain endothelial cells and epithelial cells of the choroid plexus,²⁰ suggesting that OATP1C1 compensates for MCT8 deficiency. Indeed, double knockout (DKO) of *Mct8* and *Oatp1c1* (*Slco1c1*) resembles the neuropathological changes of human MCT8 mutations, thus providing a suitable mouse model of the disease.¹⁹ The observation that the barrier-specific OATP1C1 can compensate for MCT8 deletion supports the assumption that MCT8 is critical for TH transport across the brain barriers, but definitive *in vivo* evidence is lacking.²¹

The concept that impaired TH transport through the blood–brain barrier is the primary mechanism underlying symptoms of MCT8 deficiency suggests a novel gene therapy approach, as endothelial cells of the blood–brain barrier, unlike neural cells, are

directly accessible to intravenously administered gene vectors.²² In the present study, we tested this concept in *Mct8*;*Oatp1c1* DKO mice. Our data show that adeno-associated virus (AAV)-mediated expression of *Mct8* in brain endothelial cells can prevent neurological pathology, identifying a critical role of MCT8 function in brain barriers and pointing to a new treatment strategy for AHDS patients normalizing TH levels in the CNS.

Materials and methods

Mice

As *Oatp1c1*^{-/-} and *Oatp1c1*^{+/+} mice do not differ in most parameters,²³ breeding pairs were set up among *Mct8*^{-/+};*Oatp1c1*^{-/-} and *Mct8*^{-/-};*Oatp1c1*^{-/-} mice to obtain *Mct8*^{-/-};*Oatp1c1*^{-/-} or *Mct8*^{-/+};*Oatp1c1*^{-/-} (DKO) and *Mct8*^{-/+};*Oatp1c1*^{-/-} or *Mct8*^{+/+};*Oatp1c1*^{-/-} littermate controls, as reported previously.¹⁹ Detailed information is provided in the [Supplementary material](#). Mice were randomized into treatment groups. Experimenters were blinded to group allocation in the phenotype analysis.

Statistical analysis

Sample sizes were planned based on a power analysis by G*Power. P-values ≤ 0.05 were considered statistically significant. We did not exclude outliers, unless indicated in [Supplementary Table 1](#). Outliers were identified by Grubbs test with an alpha of 0.05. ANOVA and t-test were only applied if assumptions were met, i.e. data sets were examined for Gaussian distribution using the D'Agostino–Pearson or Kolmogorov–Smirnov test, aided by visual inspection of the data, and homogeneity of variances by Brown–Forsythe test. Mostly, Holm–Sidak *post hoc* analysis was applied to test the significance between groups. For unequal variances, a Welch's ANOVA test with a Tamhane's T2 multiple comparisons *post hoc* test was used.

Study approval

All animal experiments were performed according to German animal welfare regulations and experimental protocols were approved by the local animal ethics committee (No. 11-1/17 and 97-9/19, MELUND, Kiel, Germany).

Data availability

The data that support the findings of this study are available from the corresponding author.

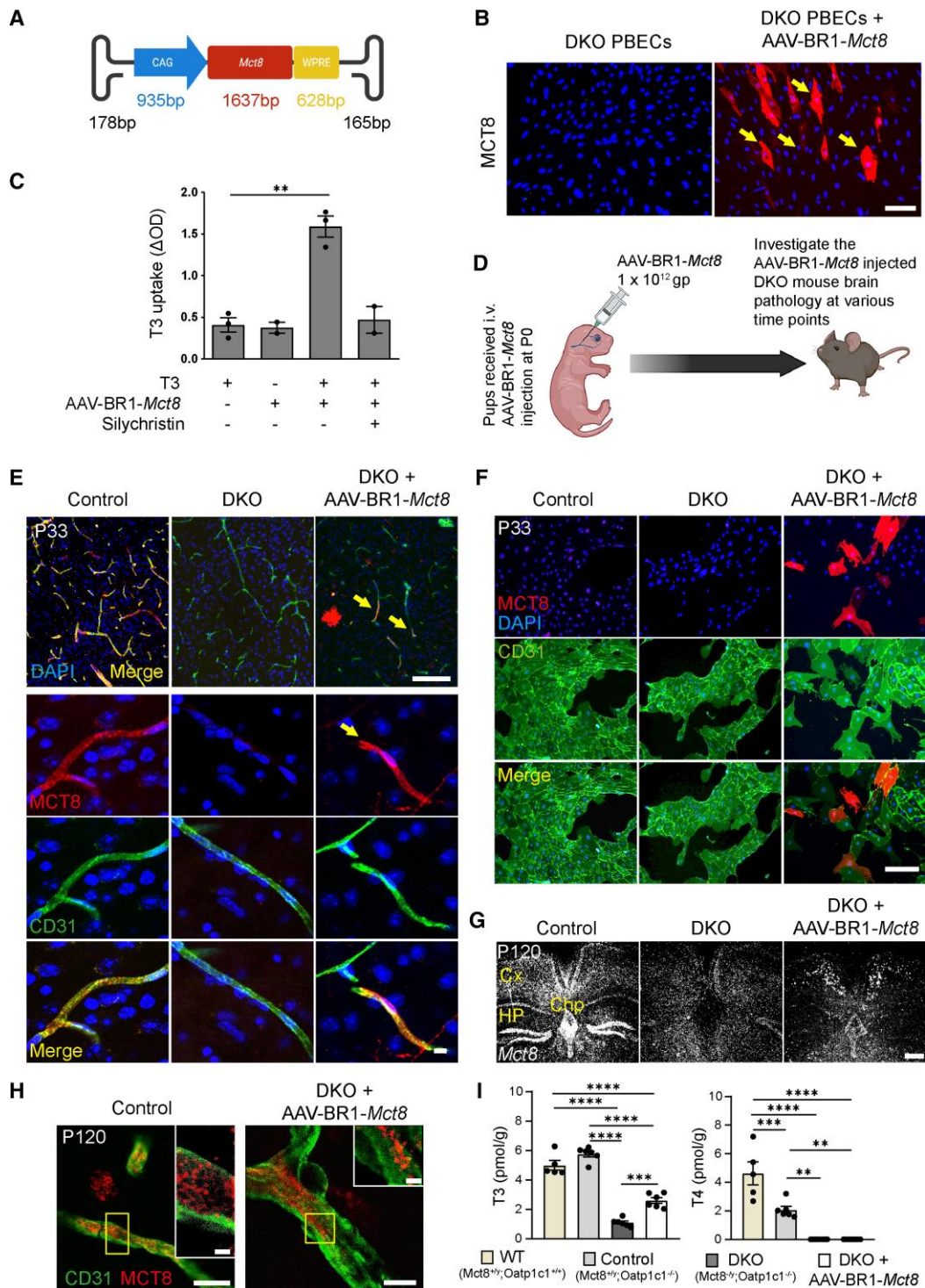


Figure 1 Intravenous administration of AAV-BR1-Mct8 enables the expression of Mct8 in brain endothelial cells and T3 transport into the CNS. (A) Schematic illustration of AAV-BR1-Mct8 vectors to transduce brain endothelial cells. CAG = cytomegalovirus enhancer fused to the chicken beta-actin promoter; WPRE = woodchuck hepatitis posttranscriptional regulatory element. (B) After transduction of primary brain endothelial cells (PBECS) of DKO mice *in vitro* with AAV-BR1-Mct8, MCT8 was expressed. MCT8 was detected by fluorescence immunostaining and nuclei with DAPI. Arrows indicate MCT8-positive cells. Scale bar = 100 μ m. (C) T3 uptake in DKO PBECS was enhanced by AAV-BR1-Mct8 treatment *in vitro*. Results were obtained from three independent cell culture preparations. ** $P = 0.0015$ (unpaired *t*-test). (D) Schematic of the experimental design, created by BioRender.com. gp = genomic particles. (E) MCT8 expression (arrow) in CD31-positive endothelial cells of control or DKO mice that received AAV-BR1-Mct8 at P0. In the top right panel, an MCT8-positive cell with the typical astrocytic morphology is visible. Fluorescence immunostaining for MCT8 and CD31 was performed at P33. Scale bars = 100 μ m; 10 μ m. (F) MCT8 expression in PBECS prepared from P33 mice that received AAV-BR1-Mct8 at P0 (MCT8-positive cells, $8.6 \pm 1.1\%$ of CD31-positive PBECS in four independent cell culture preparations, with one mouse per cell culture preparation). Scale bar = 100 μ m. (G and H) At P120, Mct8 mRNA (G) and MCT8 protein (H) were detected in control and DKO mice treated with AAV-BR1-Mct8 at P0. Insets: Higher magnification of the boxed areas. Scale bar = 100 μ m (G), 5 μ m (H), 2 μ m (insets). Cx = cortex; Chp = choroid plexus; Hp = hippocampus. (I) T3 and T4 concentrations in brains of control and DKO mice that received AAV-BR1-Mct8 at P0 and were sacrificed at P21. One-way ANOVA: T3, $F(3/19) = 104.7$, $P < 0.0001$; T4, $F(3/19) = 34.03$, $P < 0.0001$; Holm-Sidak's post hoc test. Each dot represents one animal. Means \pm SEM are shown. ** $P < 0.01$; **** $P < 0.0001$.

Results

For targeted expression of *Mct8* in the blood–brain barrier, we generated a viral *Mct8* gene vector (Fig. 1A), packaged in the AAV-BR1 capsid (AAV-BR1-*Mct8*), which selectively transduces brain endothelial cells *in vivo*.²² After incubating primary brain endothelial cells (PBECs) from *Mct8;Oatp1c1* DKO mice with AAV-BR1-*Mct8*, about 10% of the cells immunostained for MCT8, indicating transduction (Fig. 1B). To determine whether virally transduced MCT8 was functional, we measured PBEC uptake of T3. Untreated PBECs from DKO mice did not take up T3 (Fig. 1C). However, transduction of PBECs with AAV-BR1-*Mct8* enabled T3 uptake and silychristin, an MCT8 inhibitor, blocked it, confirming that MCT8 is active after viral transduction (Fig. 1C).²⁴

For *in vivo* testing, we injected AAV-BR1-*Mct8* intravenously in mice at postnatal Day 0 (P0) and investigated the animals at various time points to monitor the TH-dependent brain development and function (Fig. 1D). At P33, immunohistochemistry demonstrated robust MCT8 expression in brain endothelial cells and in some neurons and astrocytes, too, as previously described for the AAV-BR1 capsid (Fig. 1E).²² In addition, some scattered epithelial cells in the choroid plexus were transduced with *Mct8* but no tanycytes in the mediobasal hypothalamus (Supplementary Fig. 1A and B). As differentiation of endothelial cells versus pericytes or astrocyte endfeet on immunofluorescence staining can be difficult, we quantified the transduction rate of brain endothelial cells *ex vivo* by investigating PBECs derived from P33 mice that had received the vector at P0. Of PBECs derived from AAV-BR1-*Mct8*-treated mice, $8.6 \pm 1.1\%$ expressed MCT8 (Fig. 1F). However, the true transduction rate might be higher, as immunofluorescence staining sensitivity for MCT8 was limited and did not detect the downregulated endogenous MCT8 levels of cultured control cells (Fig. 1F).²⁵

In the CNS, endothelial cells are non-proliferative and quiescent after mice reach an age of 14–30 days.²⁶ Thus, loss of the non-integrating AAV vector after P33 is not expected. Accordingly, *in situ* hybridization and immunofluorescence staining showed that *Mct8* was similarly expressed in cerebral vessels of P33 and P120 DKO mice that received AAV-BR1-*Mct8* at P0 but not in other tissues, such as pituitary, kidney and liver at P21 and P120 (Fig. 1E, G and H and Supplementary Figs 1C and 2), confirming the known brain tropism of AAV-BR1 after intravenous injection.²² Importantly, targeting brain endothelial cells with AAV-BR1-*Mct8* did not impair the blood–brain barrier, nor did it induce signs of endothelial cell death (Supplementary Fig. 3).

As brain endothelial cell transduction sustained *Mct8* expression, we wondered whether it would affect TH levels in the brain. As shown previously, *Oatp1c1* deletion reduced brain T4 concentrations but had no significant effect on T3 levels, while the additional *Mct8* deletion (on an *Oatp1c1*^{-/-} background) lowered T4 and T3 concentrations (Fig. 1I).¹⁹ Importantly, AAV-BR1-*Mct8* administration to P0 DKO mice increased cerebral concentrations of the active hormone T3 but had no detectable effect on brain levels of the prohormone T4 at P21 (Fig. 1I). The lack of effect on T4 levels may be due to an enhanced metabolism of T4 to T3 in DKO mice.¹⁹ Notably, the increase in cerebral T3 levels as seen in treated DKO mice only slightly affected the hypothalamus–pituitary–thyroid (HPT) axis. *In situ* hybridization showed that *Trh* in the paraventricular nucleus and *Tshb* in the pituitary gland were not changed (Supplementary Fig. 4A).¹⁹ Moreover, treatment with AAV-BR1-*Mct8* had little effect on the elevated T3 and reduced T4 serum concentrations in DKO mice (Supplementary Fig. 4B). It slightly decreased the high expression of the TH-regulated genes

Dio1 and *Gpd2* in the liver and did not alter the reduced body weight characteristic of DKO mice (Supplementary Fig. 5A–C). The fact that AAV-BR1-*Mct8* restores *Mct8* expression in the endothelial blood–brain barrier but spares tanycytes (Supplementary Fig. 1A), the specialized glial cells that contain high amounts of MCT8 in the normal hypothalamus, might explain the lack of a marked effect on the HPT axis.¹⁶ Although AAV-BR1-*Mct8* would not completely normalize serum TH concentrations, in AHDS patients peripheral hyperthyroidism can be managed by the antithyroid drug propylthiouracil plus T4 or by TH analogues.^{12,13,27}

Supply of T3 to the brain could potentially improve neurological symptoms of MCT8 deficiency. The absence of MCT8 and OATP1C1 slows down Purkinje cell dendritogenesis.¹⁹ Consequently, the molecular layer of the cerebellum consisting of dendrites of calbindin-positive Purkinje cells was thinner in untreated P12 DKO mice than in controls (Fig. 2A). The control vector AAV-BR1-*Gfp* that encodes for the green fluorescence protein (GFP) had no effect. After injecting AAV-BR1-*Mct8*, however, the molecular layer was thicker than in untreated DKO mice (Fig. 2A) and there were more interneurons expressing the marker genes *GAD67* (glutamate decarboxylase 67) and parvalbumin in the somatosensory cortex (Fig. 2A).

AAV-BR1-*Mct8* treatment at P0 had a persistent effect. At P33, AAV-BR1-*Mct8*-treated DKO mice showed significantly thicker layers II–VI containing NeuN-positive neurons in the somatosensory cortex than untreated DKO animals (Fig. 2B). Consistent with the findings at P12, AAV-BR1-*Mct8* treatment improved *GAD67* fluorescence intensity and the number of parvalbumin-positive cells in the somatosensory cortex of DKO mice at P33 (Fig. 2B).

MRI and autopsy studies showed that myelination is abnormal or delayed in patients with MCT8 deficiency,^{14,28} reflecting the critical role of THs in postnatal myelination.⁵ At the cellular level, THs promote differentiation of oligodendrocytes that produce myelin.²⁹ As expected from the lack of THs in the CNS, DKO mice had significantly fewer Olig2-positive oligodendrocytes in the cortex and corpus callosum than controls at P33 (Fig. 3A and Supplementary Fig. 6). AAV-BR1-*Mct8* treatment at P0 significantly attenuated the decrease in Olig2-positive cells in the cortex (Fig. 3A). Under the influence of TH, oligodendrocytes produce myelin basic protein (MBP), a key component of CNS myelin.³⁰ Like human patients, DKO mice present with low MBP expression in the cortex and corpus callosum (Fig. 3B).^{14,19} However, AAV-BR1-*Mct8* treatment at P0 increased MBP levels in the cortex of DKO mice (Fig. 3B). MBP mediates myelin compaction.³¹ Accordingly, AAV-BR1-*Mct8* treatment increased levels of compact myelin in the corpus callosum as shown by FluoroMyelin staining, indicating better gross myelination (Fig. 3C). The observation that AAV-BR1-*Mct8* improved myelination was corroborated by immunoblots of the myelin proteins MBP and proteolipid protein 1 (PLP1) showing significant higher levels in DKO that received the vector at P0 (Fig. 3D and E).

To determine whether sustained *Mct8* expression affects neuronal or astrocytic function in the long term, we analysed the expression of established TH-regulated genes by using *in situ* hybridization and quantitative RT-PCR at P120. The cortical expression of hairless (*Hr*) that is known to be upregulated by THs was reduced in DKO mice at P120 (Fig. 4A)³²; AAV-BR1-*Mct8* enhanced the cortical expression of *Hr* (Fig. 4A). Moreover, the TH-regulated gene *kruppel-like factor 9* (*Klf9*) encoding a neuronal transcription factor was significantly induced by AAV-BR1-*Mct8* treatment of DKO mice (Fig. 4B). After administration of AAV-BR1-*Mct8*, expression of the TH-regulated neurogranin (*Nrgn*, *Rc3*) was slightly but non-significantly higher than in untreated DKO animals (Supplementary Fig. 7A).³³ Also, the

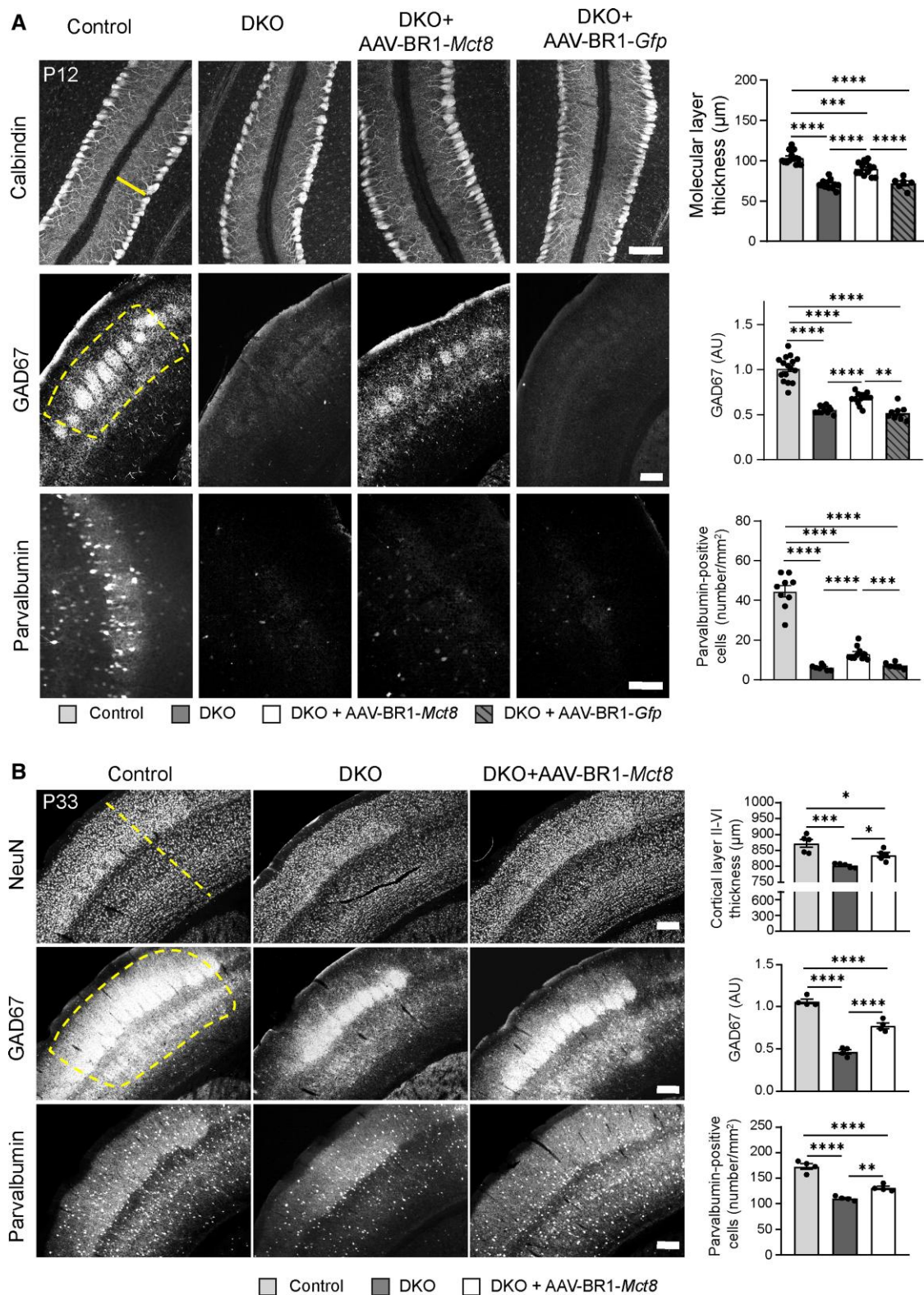


Figure 2 AAV-BR1-*Mct8* treatment improves neuronal morphology and gene expression. (A) Administration of AAV-BR1-*Mct8* at P0 to DKO mice increased thickness of the molecular layer in the cerebellar vermis as well as the relative fluorescence intensity of GAD67- and parvalbumin-positive interneurons of the somatosensory cortex at P12. Administration of AAV-BR1-*Gfp* at P0 to DKO mice had no effect. One-way ANOVA: molecular layer thickness, $F(3/40) = 50.25$, $P < 0.0001$; Holm-Sidak's post hoc test. Welch's ANOVA: GAD67, $W(3/21.43) = 58.74$, $P < 0.0001$; parvalbumin-positive interneurons, $W(3/15.37) = 64.72$, $P < 0.0001$; Tamhane's T2 post hoc test. Scale bar = 100 μm (top and bottom panel); Scale bar = 200 μm (middle panel). (B) Administration of AAV-BR1-*Mct8* at P0 improved the thickness of the somatosensory cortex layers II-VI, the relative fluorescence signal intensity of GAD67 and the number of parvalbumin-positive interneurons in the cortex at P33. One-way ANOVA: cortical thickness, $F(2/12) = 16.4$, $P = 0.0004$; GAD67, $F(2/9) = 102.0$, $P < 0.0001$; parvalbumin-positive interneurons, $F(2/9) = 63.01$, $P < 0.0001$; Holm-Sidak's post hoc test. Scale bar = 200 μm . Each dot represents one animal. Means \pm SEM are shown. Dashed line indicates region of interest. * $P < 0.05$; ** $P < 0.01$; *** $P < 0.001$; **** $P < 0.0001$.

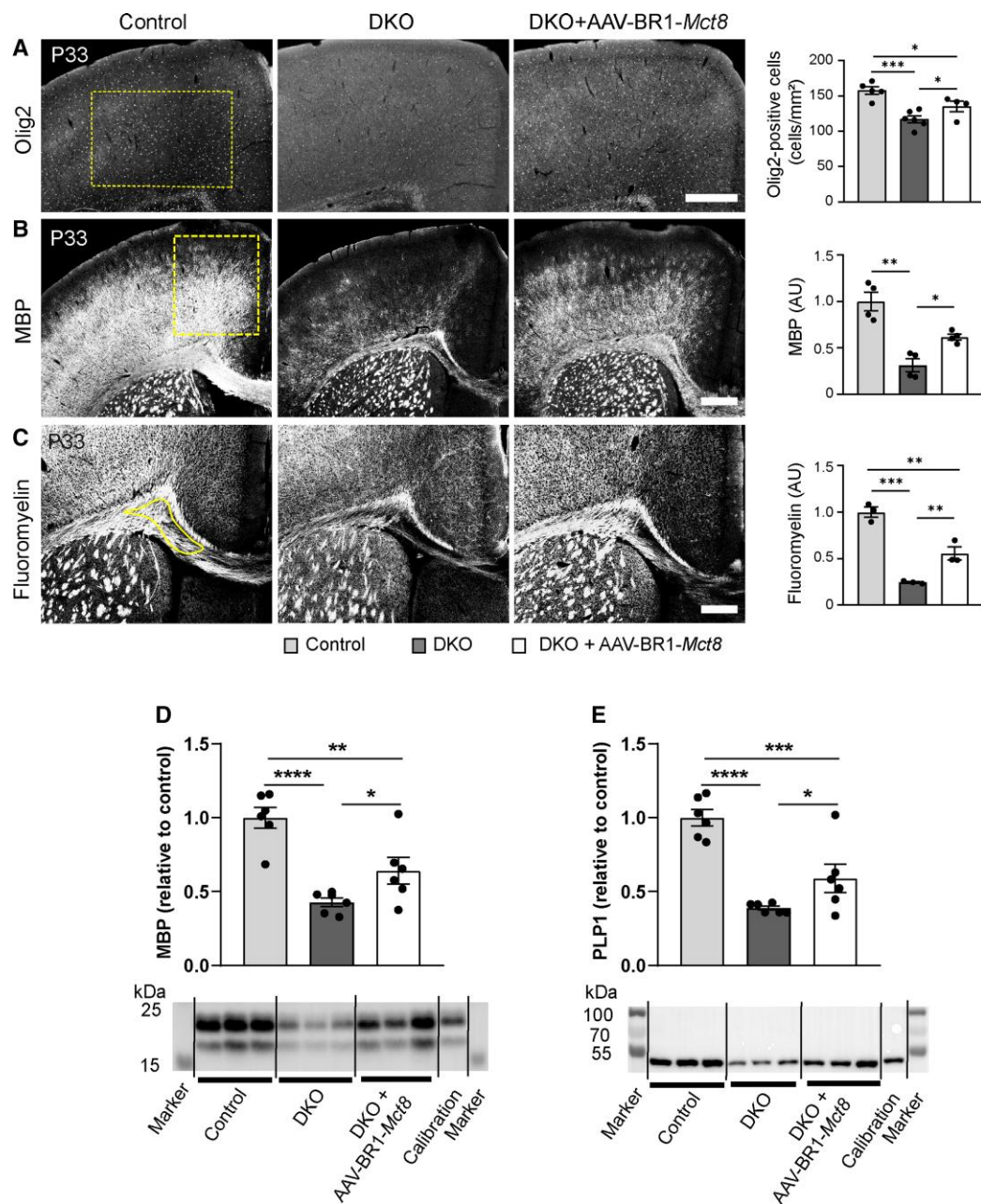


Figure 3 AAV-BR1-Mct8 treatment increases oligodendrocyte numbers and myelination. Treatment of DKO mice at P0 improved several parameters of myelination at P33 and P21. (A) The reduced number of Olig2-immunopositive oligodendrocytes in the cerebral cortex was significantly increased in DKO treated with AAV-BR1-Mct8 at P33. Scale bar = 200 μ m. One-way ANOVA, $F(2/12) = 13.94$, $P = 0.0007$; Holm-Sidak's post hoc test. (B) AAV-BR1-Mct8 improved MBP levels in the cortex of DKO mice at P33. MBP was detected by immunostaining. Scale bar = 100 μ m. Welch's ANOVA test, $W(2/4.96) = 14.8$, $P = 0.0081$; Tamhane's T2 post hoc test. (C) Compact myelin stained by FluoroMyelin was diminished in the corpus callosum of untreated DKO but improved by treatment with AAV-BR1-Mct8 at P33. Scale bar = 100 μ m. One-way ANOVA, $F(2/6) = 53.15$, $P = 0.0002$; Holm-Sidak's post hoc test. (D and E) AAV-BR1-Mct8 treatment at P0 increased the levels of MBP (D) and PLP1 (E) in brain lysate of DKO mice at P21 as determined by immunoblotting. One-way ANOVA: MBP, $F(2/15) = 18.09$, $P = 0.0001$; PLP1, $F(2/15) = 23.05$, $P < 0.0001$; Holm-Sidak's post hoc test. Cropped blots are shown; for full-length blots, see [Supplementary Fig. 8](#). Each dot represents one animal. Means \pm SEM are shown. Dashed line indicates region of interest. * $P < 0.05$; ** $P < 0.01$; *** $P < 0.001$; **** $P < 0.0001$.

reduced levels of aldehyde dehydrogenase 1a1 (*Aldh1a1*), a TH-dependent gene expressed mainly in astrocytes and fibroblasts, were elevated by AAV-BR1-Mct8 (Fig. 4C).^{19,34} In contrast to the four previous genes that are induced by THs, the mRNA of the astrocytic deiodinase 2 (*Dio2*) that converts T4 into T3 was increased in the cortex of DKO and AAV-BR1-Mct8 had no significant effect on the expression level (Fig. 4D). Thus, the findings

demonstrate that AAV-BR1-Mct8 treatment at P0 has a long-lasting effect on the expression of several TH-dependent neuronal and astrocytic genes.

MCT8-deficient patients suffer from coordination deficits.⁹ Like AHDS patients, DKO mice exhibited locomotor deficiencies, including impaired motor coordination and learning in comparison to littermate controls when investigated in the rotarod test at P120

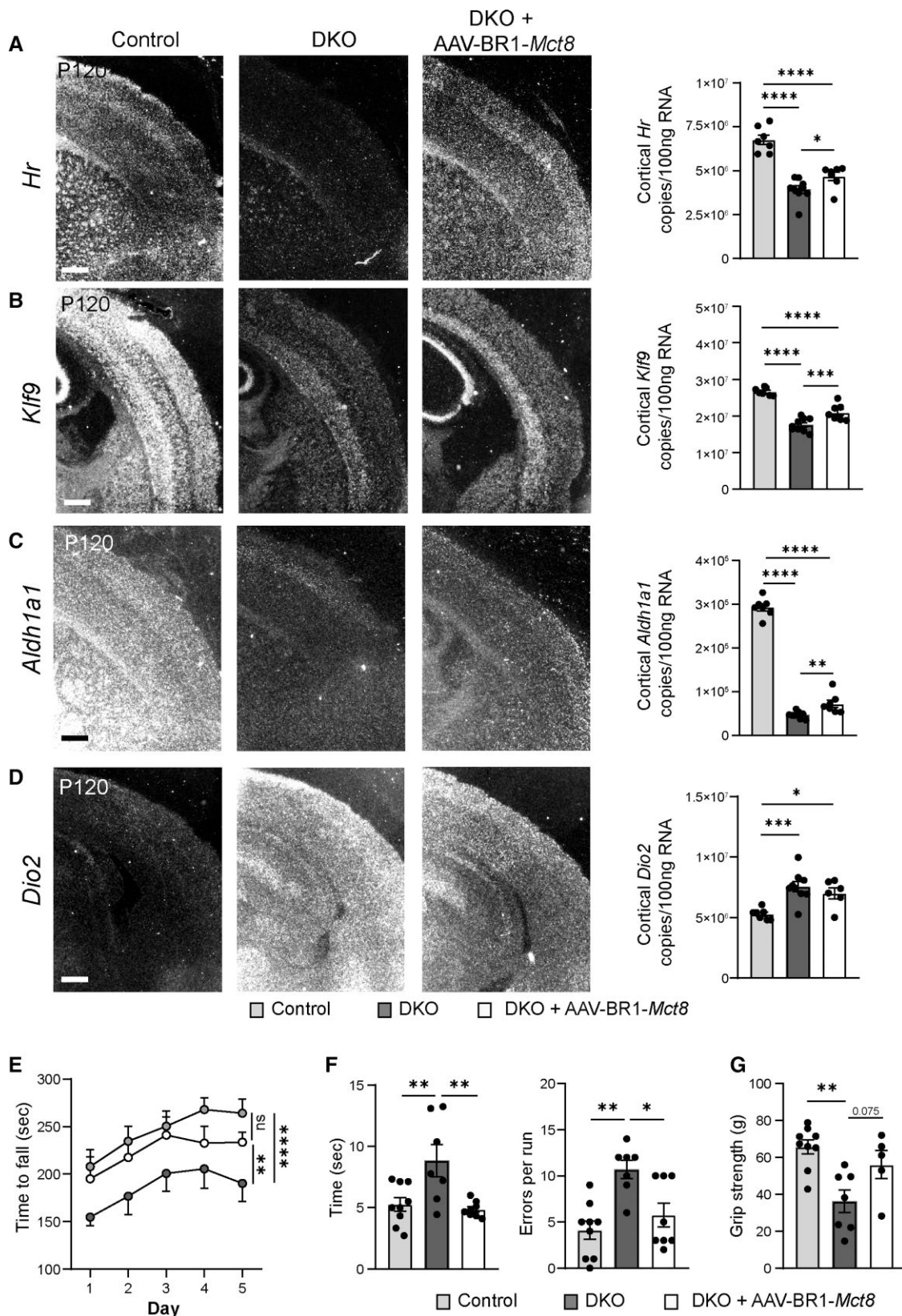


Figure 4 AAV-BR1-Mct8 treatment improves expression of TH-dependent genes and motor function in DKO mice. (A and B) AAV-BR1-Mct8 injected at P0 increased the expression of neuronal *Hr* and *Klf9* in the cortex of DKO mice at P120. Gene expression was visualized by in situ hybridization and quantified by qPCR. In situ hybridization images are representative for several replicates (Supplementary Table 1). Scale bar = 100 μ m. One-way ANOVA: *Hr*, $F(2/20) = 36.92$, $P < 0.0001$; *Klf9*, $F(2/20) = 52.79$, $P < 0.0001$; Holm-Sidak's post hoc test. (C and D) AAV-BR1-Mct8 injected at P0 increased the expression of astrocytic *Aldh1a1* (C) in the cortex of DKO mice at P120. The elevated cortical *Dio2* expression (D) in DKO mice was not reduced by AAV-BR1-Mct8.

(Continued)

(Fig. 4E).¹⁹ However, a single intravenous injection of AAV-BR1-Mct8 at P0 significantly improved DKO mice performance in the rotarod test (Fig. 4E). In the beam walk, another test of coordination and balance, DKO mice treated with AAV-BR1-Mct8 crossed the beam faster than untreated DKO and made fewer errors (Fig. 4F). Moreover, grip strength tended to be greater in AAV-BR1-Mct8-treated DKO mice (Fig. 4G).

If there are no other known cases in the family, AHDS is typically diagnosed with some delay, precluding a therapeutic intervention early after birth.⁹ To determine whether AAV-BR1-Mct8 would also improve the phenotype when administered at a juvenile age, we treated DKO mice at P30 with an intravenous injection of AAV-BR1-Mct8 (Fig. 5A). At P51, many capillaries throughout the brain of AAV-BR1-Mct8-treated DKO mice expressed MCT8 (Fig. 5B). In addition, a few neurons and astrocytes were transduced. Intriguingly, AAV-BR1-Mct8 markedly corrected the aberrant expression of the TH-dependent genes *Klf9*, *Hr*, *Aldh1a1* and *Dio2* and even normalized mRNA levels of *Klf9*, *Aldh1a1* and *Dio2* (Fig. 5C). Likewise, AAV-BR1-Mct8 corrected the thickness of the cortical layers II–VI and of the molecular layer in the cerebellum (Fig. 5D and G). The gene therapy increased the expression of the interneuron marker GAD67 and the number of parvalbumin-positive interneurons in the somatosensory cortex (Fig. 5E and F). The effect of AAV-BR1-Mct8 on myelin markers was more variable with a normalization of the number of Olig2-positive oligodendrocytes in the corpus callosum and a trend towards more Olig2 protein as determined by immunoblot but no significant effect on MBP levels (Fig. 5H–J). The number of mature CC1-positive oligodendrocytes was also not altered by this treatment regime (Supplementary Fig. 6B). Overall, the data show that AAV-BR1-Mct8, even when administered at a juvenile age, ameliorates deficits in neural gene expression and brain structure, while effects on myelination were more variable and may require more time to fully develop.

Discussion

Our study reports a novel gene therapy for MCT8 deficiency, a major cause of X-linked intellectual disability. Previous investigations expressed MCT8 in mice with the help of the AAV9 capsid.^{35,36} After intracerebroventricular injection of the vector, expression in parenchymal cells did not correct low TH concentrations in the brain, presumably because the blood–brain barrier transport of THs was still compromised.³⁵ In contrast, when the AAV9 vector was intravenously injected at P30, it ameliorated the phenotype of DKO mice.³⁶ However, the latter study did not investigate the efficacy of an earlier administration or the cellular expression of MCT8.³⁶ In general, AAV9 is known for its unspecific tropism. It crosses the blood–brain barrier and transduces neural cells and epithelial cells of the choroid plexus, complicating the mechanistic interpretation of the latter study. Moreover, transduction of extraneural cells, such as hepatocytes, may cause potentially severe side effects.^{37,38} In the present study, targeting the small endothelial cell population was

sufficient to supply T3 to the brain and to improve symptoms of MCT8 deficiency in a mouse model. Thus, the data confirm that endothelial cells are a critical site for postnatal MCT8 function.

Assuming that permeation into the brain is the key problem in MCT8 deficiency, previous studies have attempted to circumvent the blood–brain barrier by administering TH or TH analogues intranasally or intracerebroventricularly, but with limited success.^{9,39,40} Apparently, endothelial MCT8 is highly efficient in supplying the CNS with TH. After THs enter the CNS through MCT8, uptake in glia or neurons may occur through other transporters, including MCT10, L-type amino acid transporters (LATs), or OATP1C1.⁶

Normal brain development requires TH action already before birth, but how THs cross the prenatal blood–brain barrier is still unclear. Human brain vessels express MCT8 already at gestational Week 14.¹⁵ Lower brain TH concentrations in an MCT8-deficient foetus suggest that MCT8 plays a role in foetal TH transport.¹⁴ On the other hand, patients with MCT8 deficiency are normal at birth and only develop symptoms during the first year of life.^{7,8,28} Our study now provides functional data that postnatal reconstitution of MCT8 is sufficient to prevent the neurological phenotype of the disease, at least partially.

MCT8 expression could be directed to the neonatal or juvenile blood–brain barrier by using an AAV vector with high selectivity for brain endothelial cells.²² This approach improved transcriptional and morphological parameters of the disease already after 12 days. Importantly, the effect persisted at the behavioural and transcriptional level into adulthood. Thus, brain endothelial cell-specific gene therapy emerges as a potential novel treatment of the disabling neurological signs of AHDS. Before the approach is translated into the clinic, several aspects have to be considered. First, it should be noted that the concept is based on a mouse model, the validity of which is open to challenge. The example of *Oatp1c1* shows that there are species differences in the transport of THs.⁶ Even on an *Oatp1c1*-deficient background, the phenotype of *Mct8* deficiency seems to be less severe in mice than in humans.⁹ It is possible that during human development, transient expression of MCT8 by neurons and neural precursor cells or the low expression in adult neural cells contribute to MCT8 function.^{17,41–43} Second, it will be important to see whether AAV-BR1 possesses the same tropism for brain endothelial cells in humans as in mice. Recently, another AAV capsid, AAV-BI30, has been reported to target brain endothelial cells in mice after intravenous injection, providing an alternative to implement the gene therapy strategy developed here.⁴⁴ Despite the rather low transduction rate of brain endothelial cells in our mouse model, the marked effects are reassuring and suggest that the transduction rate must not be high to achieve a therapeutic benefit in humans. Finally, the therapeutic time window has to be defined because MCT8 deficiency is often diagnosed with some delay. In this respect, it is important that treatment with AAV-BR1-Mct8 was still effective when initiated at a juvenile age (P30). Overall, we believe that brain endothelial targeting could be a valuable strategy to treat AHDS.

Figure 4 Continued

Scale bar = 100 μ m. One-way ANOVA: *Aldh1a1*, $F(2/20) = 440.4$, $P < 0.0001$; *Dio2*, $F(2/19) = 10.01$, $P = 0.0011$; Holm–Sidak's post hoc test. (E) AAV-BR1-Mct8 treatment at P0 prolonged the time DKO mice were able to balance on the rotarod as a sign of improved coordination and motor learning. Mice were assessed on five consecutive days starting at P120. Repeated-measures ANOVA, $F(2/26) = 5.045$, $P = 0.0141$; Holm–Sidak's post hoc test. (F) AAV-BR1-Mct8 treatment reduced the time DKO mice needed to cross the beam and led to a trend towards fewer errors, indicating better motor coordination. One-way ANOVA: time, $F(2/21) = 7.567$, $P = 0.0034$; errors, $F(2/21) = 9.274$, $P = 0.0013$; Holm–Sidak's post hoc test. (G) AAV-BR1-Mct8 treatment tended to increase the grip strength of DKO mice in comparison to control animals. One-way ANOVA, $F(2/18) = 8.301$, $P = 0.0028$; Holm–Sidak's post hoc test. Each dot represents one animal. Means \pm SEM are shown. ns = non-significant; * $P < 0.05$; ** $P < 0.01$; *** $P < 0.001$; **** $P < 0.0001$.

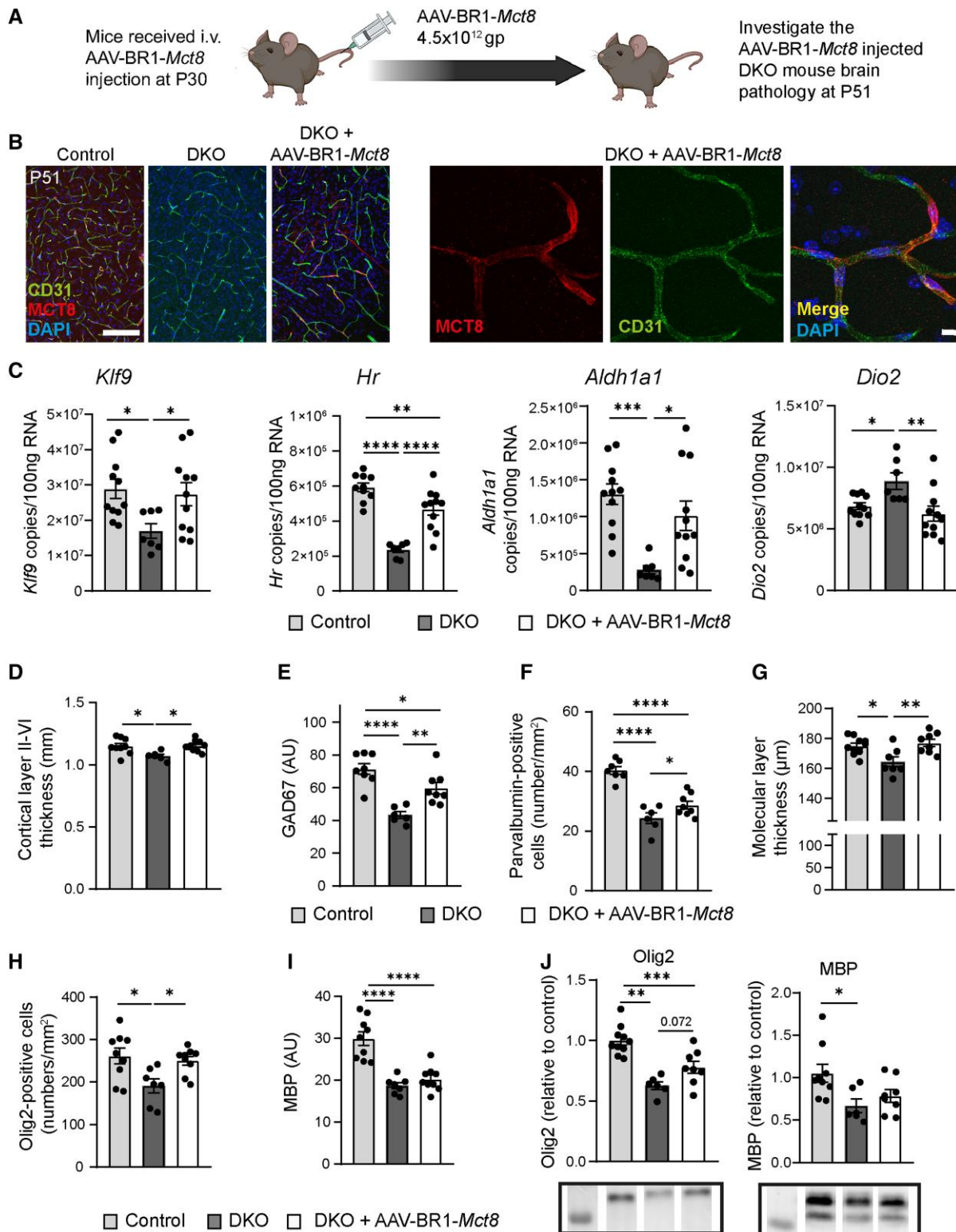


Figure 5 Intravenous administration of AAV-BR1-*Mct8* in juvenile mice enables the expression of *Mct8* in brain endothelial cells and improves T3-dependent parameters. (A) Schematic of the experimental design, created by BioRender.com. gp = genomic particles. (B) MCT8 expression in CD31-positive endothelial cells of control or DKO mice that received AAV-BR1-*Mct8* at P30. Fluorescence immunostaining for MCT8 and CD31 was performed at P51. Scale bar = 100 μm (left), 10 μm (right). (C) AAV-BR1-*Mct8* injected at P30 increased the expression of *Klf9*, *Hr* and *Aldh1a1* and reduced expression of *Dio2* in DKO mice at P51. Gene expression was quantified by qPCR. One-way ANOVA: *Klf9*, $F(2/26) = 4.031$, $P = 0.0299$; *Hr*, $F(2/25) = 32.80$, $P < 0.0001$; *Aldh1a1*, $F(2/26) = 8.9$, $P = 0.0011$; *Dio2*, $F(2/26) = 6.076$, $P = 0.0068$; Holm-Sidak's post hoc test. (D–G) Administration of AAV-BR1-*Mct8* at P30 improved the thickness of the somatosensory cortex layers II–VI (D), the relative fluorescence signal intensity of GAD67 (E), the number of parvalbumin-positive interneurons (F) and the thickness of the molecular layer in the cerebellar vermis (G) at P51. One-way ANOVA for cortical thickness, $F(2/22) = 5.723$,

(Continued)

Figure 5 Continued

$P = 0.0099$; GAD67, $F(2/19) = 17.75$, $P < 0.0001$; parvalbumin, $F(2/18) = 31.46$, $P < 0.0001$; molecular layer thickness, $F(2/22) = 6.723$, $P = 0.0053$; Holm–Sidak's *post hoc* test. (H) The reduced number of Olig2-immunopositive oligodendrocytes in the corpus callosum was significantly increased in DKO treated with AAV-BR1-Mct8. One-way ANOVA, $F(2/22) = 12.74$, $P = 0.0002$; Holm–Sidak's *post hoc* test. (I) AAV-BR1-Mct8 did not improve MBP levels of DKO mice. MBP was detected by immunostaining. One-way ANOVA, $F(2/22) = 23.95$, $P < 0.0001$; Holm–Sidak's *post hoc* test. (J) Protein levels of Olig2 and MBP quantified by immunoblot were not improved compared with DKO mice. One-way ANOVA: Olig2, $F(2/21) = 19.31$, $P < 0.0001$; MBP, $F(2/20) = 4.523$, $P = 0.024$; Holm–Sidak's *post hoc* test. Each dot represents one animal. Means \pm SEM are shown. Cropped blots are shown; for the full-length blots, see [Supplementary Fig. 9](#). * $P < 0.05$; ** $P < 0.01$; *** $P < 0.001$; **** $P < 0.0001$.

Acknowledgements

We thank Ines Stöling, Wiebke Brandt, Beate Lembrich, Frauke Spiecker (Pharmacology), Julia Resch (Institute for Endocrinology and Diabetes) and Christian L. Schmidt (Isotope laboratory) for their kind support.

Funding

This work was supported by the European Research Council (ERC) Synergy Grant-2019-WATCH-810331 to V.P., R.N. and M.S., by grants of the Deutsche Forschungsgemeinschaft (MU-3743/1-1 to H.M.F., CRC/TR296 to H.M.F., T.M., H.H., J.M. and M.S.) and by the Sherman family funds to H.H.

Competing interests

The authors report no competing interests.

Supplementary material

[Supplementary material](#) is available at [Brain online](#).

References

- Wood-Allum CA, Shaw PJ. Thyroid disease and the nervous system. *Handb Clin Neurol*. 2014;120:703–735.
- Halpern JP, Boyages SC, Maberly GF, Collins JK, Eastman CJ, Morris JG. The neurology of endemic cretinism. A study of two endemias. *Brain*. 1991;114(Pt 2):825–841.
- Dwyer JB, Aftab A, Radhakrishnan R, et al. Hormonal treatments for major depressive disorder: State of the art. *Am J Psychiatry*. 2020;177:686–705.
- Tan ZS, Vasan RS. Thyroid function and Alzheimer's disease. *J Alzheimers Dis*. 2009;16:503–507.
- Bernal J, Guadano-Ferraz A, Morte B. Thyroid hormone transporters—Functions and clinical implications. Review. *Nat Rev Endocrinol*. 2015;11:406–417.
- Groeneweg S, van Geest FS, Peeters RP, Heuer H, Visser WE. Thyroid hormone transporters. *Endocr Rev*. 2020;41:bnz008. doi:10.1210/edrev/bnz008
- Friesema EC, Grueters A, Biebermann H, et al. Association between mutations in a thyroid hormone transporter and severe X-linked psychomotor retardation. *Lancet*. 2004;364:1435–1437.
- Dumitrescu AM, Liao XH, Best TB, Brockmann K, Refetoff S. A novel syndrome combining thyroid and neurological abnormalities is associated with mutations in a monocarboxylate transporter gene. *Am J Hum Genet*. 2004;74:168–175.
- Krude H, Biebermann H, Schuelke M, Müller TD, Tschöp M. Allan–Herndon–Dudley syndrome: Considerations about the brain phenotype with implications for treatment strategies. *Exp Clin Endocrinol Diabetes*. 2020;128:414–422.
- Schwartz CE, May MM, Carpenter NJ, et al. Allan–Herndon–Dudley syndrome and the monocarboxylate transporter 8 (MCT8) gene. *Am J Hum Genet*. 2005;77:41–53.
- Visser WE, Vrijmoeth P, Visser FE, Arts WF, van Toor H, Visser TJ. Identification, functional analysis, prevalence and treatment of monocarboxylate transporter 8 (MCT8) mutations in a cohort of adult patients with mental retardation. *Clin Endocrinol (Oxf)*. 2013;78:310–315.
- Groeneweg S, Peeters RP, Moran C, et al. Effectiveness and safety of the tri-iodothyronine analogue TRIAC in children and adults with MCT8 deficiency: An international, single-arm, open-label, phase 2 trial. *Lancet Diabetes Endocrinol*. 2019;7:695–706.
- Verge CF, Konrad D, Cohen M, et al. Diiodothyropropionic acid (DITPA) in the treatment of MCT8 deficiency. *J Clin Endocrinol Metab*. 2012;97:4515–4523.
- Lopez-Espindola D, Morales-Bastos C, Grijota-Martinez C, et al. Mutations of the thyroid hormone transporter MCT8 cause prenatal brain damage and persistent hypomyelination. *J Clin Endocrinol Metab*. 2014;99:E2799–E2804.
- Lopez-Espindola D, Garcia-Aldea A, Gómez de la Riva I, et al. Thyroid hormone availability in the human fetal brain: Novel entry pathways and role of radial glia. *Brain Struct Funct*. 2019;224:2103–2119.
- Wilpert NM, Krueger M, Opitz R, et al. Spatiotemporal changes of cerebral monocarboxylate transporter 8 expression. *Thyroid*. 2020;30:1366–1383.
- Alkemade A, Friesema EC, Unmehopa UA, et al. Neuroanatomical pathways for thyroid hormone feedback in the human hypothalamus. *J Clin Endocrinol Metab*. 2005;90:4322–4334.
- Trajkovic M, Visser TJ, Mittag J, et al. Abnormal thyroid hormone metabolism in mice lacking the monocarboxylate transporter 8. *J Clin Invest*. 2007;117:627–635.
- Mayerl S, Müller J, Bauer R, et al. Transporters MCT8 and OATP1C1 maintain murine brain thyroid hormone homeostasis. *J Clin Invest*. 2014;124:1987–1999.
- Roberts LM, Woodford K, Zhou M, et al. Expression of the thyroid hormone transporters monocarboxylate transporter-8 (SLC16A2) and organic ion transporter-14 (SLCO1C1) at the blood–brain barrier. *Endocrinology*. 2008;149:6251–6261.
- Vatine GD, Al-Ahmad A, Barriga BK, et al. Modeling psychomotor retardation using iPSCs from MCT8-deficient patients indicates a prominent role for the blood–brain barrier. *Cell Stem Cell*. 2017;20:831–843.e5.
- Körbelin J, Dogbevia G, Michelfelder S, et al. A brain microvasculature endothelial cell-specific viral vector with the potential to treat neurovascular and neurological diseases. *EMBO Molecular Medicine*. 2016;8:609–625.
- Mayerl S, Visser TJ, Darras VM, Horn S, Heuer H. Impact of Oatp1c1 deficiency on thyroid hormone metabolism and action in the mouse brain. *Endocrinology*. 2012;153:1528–1537.
- Johannes J, Jayarama-Naidu R, Meyer F, et al. Silychristin, a flavonolignan derived from the milk thistle, is a potent inhibitor of the thyroid hormone transporter MCT8. *Endocrinology*. 2016;157:1694–1701.
- Sabbagh MF, Nathans J. A genome-wide view of the de-differentiation of central nervous system endothelial cells in culture. *Elife*. 2020;9:e51276.

26. Harb R, Whiteus C, Freitas C, Grutzendler J. In vivo imaging of cerebral microvascular plasticity from birth to death. *J Cereb Blood Flow Metab.* 2013;33:146–156.
27. Wemeau JL, Pigeyre M, Proust-Lemoine E, et al. Beneficial effects of propylthiouracil plus L-thyroxine treatment in a patient with a mutation in MCT8. *J Clin Endocrinol Metab.* 2008;93:2084–2088.
28. Groeneweg S, van Geest FS, Abaci A, et al. Disease characteristics of MCT8 deficiency: An international, retrospective, multi-centre cohort study. *Lancet Diabetes Endocrinol.* 2020;8:594–605.
29. Barres BA, Lazar MA, Raff MC. A novel role for thyroid hormone, glucocorticoids and retinoic acid in timing oligodendrocyte development. *Development.* 1994;120:1097–1108.
30. Farsetti A, Mitsuhashi T, Desvergne B, Robbins J, Nikodem VM. Molecular basis of thyroid hormone regulation of myelin basic protein gene expression in rodent brain. *J Biol Chem.* 1991;266:23226–23232.
31. Readhead C, Popko B, Takahashi N, et al. Expression of a myelin basic protein gene in transgenic shiverer mice: Correction of the dysmyelinating phenotype. *Cell.* 1987;48:703–712.
32. Potter GB, Zarach JM, Sisk JM, Thompson GC. The thyroid hormone-regulated corepressor hairless associates with histone deacetylases in neonatal rat brain. *Mol Endocrinol.* 2002;16:2547–2560.
33. Iniguez MA, Rodriguez-Pena A, Ibarrola N, Morreale de Escobar G, Bernal J. Adult rat brain is sensitive to thyroid hormone. Regulation of RC3/neurogranin mRNA. *J Clin Invest.* 1992;90:554–558.
34. Vanlandewijck M, He L, Mae MA, et al. A molecular atlas of cell types and zonation in the brain vasculature. *Nature.* 2018;554:475–480.
35. Iwayama H, Liao XH, Braun L, et al. Adeno associated virus 9-based gene therapy delivers a functional monocarboxylate transporter 8, improving thyroid hormone availability to the brain of Mct8-deficient mice. *Thyroid.* 2016;26:1311–1319.
36. Liao XH, Avalos P, Shelest O, et al. AAV9-MCT8 delivery at juvenile stage ameliorates neurological and behavioral deficits in a mouse model of MCT8-deficiency. *Thyroid.* Published online 20 May 2022. doi:10.1089/thy.2022.0034
37. Walia JS, Altaleb N, Bello A, et al. Long-term correction of Sandhoff disease following intravenous delivery of rAAV9 to mouse neonates. *Mol Ther.* 2015;23:414–422.
38. Chand D, Mohr F, McMillan H, et al. Hepatotoxicity following administration of onasemnogene abeparvovec (AVXS-101) for the treatment of spinal muscular atrophy. *J Hepatol.* 2021;74:560–566.
39. Báñez-López S, Grijota-Martínez C, Liao X-H, Refetoff S, Guadaño-Ferraz A. Intracerebroventricular administration of the thyroid hormone analog TRIAC increases its brain content in the absence of MCT8. *PLoS One.* 2019;14:e0226017.
40. Grijota-Martínez C, Báñez-López S, Ausó E, Refetoff S, Frey WH, Guadaño-Ferraz A. Intranasal delivery of thyroid hormones in MCT8 deficiency. *PLoS One.* 2020;15:e0236113.
41. Zhang Y, Sloan SA, Clarke LE, et al. Purification and characterization of progenitor and mature human astrocytes reveals transcriptional and functional differences with mouse. *Neuron.* 2016;89:37–53.
42. Vatine GD, Shelest O, Barriga BK, et al. Oligodendrocyte progenitor cell maturation is dependent on dual function of MCT8 in the transport of thyroid hormone across brain barriers and the plasma membrane. *Glia.* 2021;69:2146–2159.
43. Chan SY, Hancox LA, Martin-Santos A, et al. MCT8 Expression in human fetal cerebral cortex is reduced in severe intrauterine growth restriction. *J Endocrinol.* 2014;220:85–95.
44. Krolak T, Chan KY, Kaplan L, et al. A high-efficiency AAV for endothelial cell transduction throughout the central nervous system. *Nat Cardiovasc Res.* 2022;1:389–400.